RSC Advances

Journal Name

COMMUNICATION

EDC/NHS activation mechanism of polymethacrylic acid: anhydride versus NHS-ester

Qin Yan,[a] Hong-Ning Zheng,[a] Chuan Jiang,[a] Kun Li,[a] and Shou-Jun Xiao*[a]

Polymer brushes of polymethacrylic acid (PMAA) and PMAA-associated polymer blends of PMAA/PNIPAM (poly-N-isopropylacrylamide) were prepared on porous silicon for further investigation of the EDC/NHS (1-ethyl-3-(3-dimethylaminopropyl)carbodiimide/N-hydroxysuccinimide) activation mechanisms by infrared spectroscopy. With increasing the fragmentation degree of PMAA blocks in PMAA-associated polymer blends, the product of anhydride wanes from dominant to recessive, whereas a complementary product of NHS-ester waxes from recessive to dominant. The Thorpe-Ingold effect was applied to explain the formation of anhydride, that the gem-dialkyl groups of PMAA next to carboxylic acids compress the acid side chains close to each other, once the intermediate of O-acylisourea forms, it will be attacked by the intramolecular neighboring acid much faster than any other nucleophiles such as NHS and water, therefore the six-membered ring of anhydride forms. All acid side chains in PMAA standing next to each other will form anhydride primarily due to the Thorpe-Ingold effect, unless they are sterically hindered, whereas only the lonely acid side chains isolated by others, form NHS-ester. The EDC/NHS activation results of four small molecules of dicarboxylic acids in aqueous media, glutaric acid and 2,2-dimethyl glutaric acid generating disuccinimidyl ester with high yield, succinic acid and 2,2-dimethyl succinic acid remain intact, can also be explained by the Thorpe-Ingold effect. The clear understanding of the EDC/NHS activation mechanisms of PMAA will be a step closer to resolve the mechanistic ambiguity of the carbodiimide/additive coupling reactions for amide bond formation.

RSC Advances Accepted Manuscript

Introduction

Amide bond formation (or amidation) from carboxylic acid by carbodiimide activation with the assistance of additives such as NHS, then addition of amine sequentially in one-pot or in stepwise reactions, is so broadly used in peptide synthesis, bio-conjugation, immunochemistry, biosensing, etc., that it would be hard to overstate its importance.[1] However the reaction mechanisms still remain challenging,[2] especially with debates on the intermediates, and a direct evidence is the large deviation of product yields for very similar carboxylic acids under the same reaction conditions. The initial activation intermediate is undoubtedly believed to be the unstable O-acylisourea,[3] which goes through several transition routes and mechanisms to stable intermediates or byproducts, the focal point for debating. Taking one of the most common activation recipes as an example, EDC and an additive of NHS or sulfo-NHS with carboxylic acid in aqueous media, the initial intermediate of O-acylisourea converts to stable intermediates or byproducts through the following 4 pathways: 1st, nucleophilic addition of NHS to generate NHS-ester, which forms amide with amine in a weak alkaline solution at room temperature efficiently; 2nd, nucleophilic addition of carboxylic acid to form symmetrical anhydride (suggested but a stable anhydride intermediate in aqueous media was only captured and confirmed recently in the PMAA system by us[4]), which can react with amine directly to amide, or with nucleophilic addition of NHS to NHS-ester, or by hydrolysis to carboxylic acid; 3rd, rearrangement to a stable side product of N-acyl urea; 4th, hydrolysis to urea and carboxylic acid by consuming carbodiimide only. All the above pathways make an individual acid to the product of amide complicated, for the reason in dealing with the thermodynamics and kinetics of different pathways.[5]

In our previous report,[4b] two different intermediates were observed in two similar acid polymers respectively after EDC/NHS activation, NHS-ester from polyacrylic acid which is normal, while anhydride from PMAA which is a surprise. We interpreted the capture of polymethacrylic anhydride with two reasons: the faster kinetic intra-molecular nucleophilic attack of carboxylic acid from a neighboring side chain to O-acylisourea than any other pathways and the stable thermodynamic structure of polymethacrylic anhydride to avoid further nucleophilic attack from NHS and water. Similar to NHS-ester, polymethacrylic anhydride, a good bioconjugate reagent, possesses a longer shelf life time and bears the metastability towards hydrolysis over hours in weak alkaline solutions. Obviously, both kinetic and thermodynamic properties of PMAA during the EDC/NHS activation relate to the side chains of methyl groups, which is specifically called the Thorpe-Ingold effect (or gem-dialkyl effect), one of the neighboring group effects.[6] The stable intermediate anhydride structure captured renders PMAA so special that further investigation on the EDC/NHS activation of PMAA and polyacrylic acid (PAA) will be not only beneficial for practical applications but also for understanding the carbodiimide-triggered amidation mechanisms better.

In this work, we have investigated the EDC/NHS activation of two PMAA-based polymer brushes grafted on porous silicon:[4b,7] 1) reiterative EDC/NHS activation and amidation of PMAA brushes, 2) EDC/NHS activation of the polymer blend brushes of PMAA/PNIPAM (poly-N-isopropylacrylamide) grown from mixed monomers of methacrylic acid (MAA) and N-isopropylacrylamide

(NIPAM) with blending ratios of 10, 20, 30, 40, 50, 60, 70, 80, 90, and 100% MAA. We adapted our previous method:[4b] infrared measurements of stepwise surface reactions, which possess the merit of ignoring the laborious separation and purification procedure, especially for multiple reaction steps in aqueous media. 3-Amino-1-azidopropane (AAP),[8] an infrared probe of the azido tag with a strong stretching band at 2105 cm^{-1}, was used as the amidation reagent. We observed the complementary waxing of NHS-ester and waning of anhydride with increasing the fragmentation degree of PMAA blocks in the above-mentioned two polymer systems after EDC/NHS activation. Anhydride evolves from dominant to recessive, while NHS-ester from recessive to dominant complementarily with all-neighboring acid side chains to isolated ones by inserting other side chains. Further amidation kinetics for both PMAA anhydride and NHS-ester with AAP by means of the infrared absorption evolution against the reaction time was investigated. Finally the Thorpe-Ingold effect was applied to interpret the EDC/NHS activation of 4 small dicarboxylic acids of glutaric acid, 2,2-dimethyl glutaric acid, 2,2-dimethyl succinic acid, and succinic acid. All the experimental results helped us to speculate that the faster nucleophilic attack on O-acylisourea for PMAA, 2,2-dimethyl succinic acid, and succinic acid is from the intramolecular neighboring acid due to the Thorpe-Ingold effect, thus generating anhydride; whereas the faster nucleophilic attack on O-acylisourea for PAA, glutaric acid, and 2,2-dimethyl glutaric acid is from the intermolecular NHS, therefore producing NHS-ester.

Experimental Section

Materials

Single-side polished silicon wafers (<100>, p-type, boron-doped, 5.0–8.0 Ω.cm, 500 μm thick) were purchased from Hefei Kejing Materials Technology CO. LTD. N-Ethyl-N'-(3-(dimethylamino)propyl)carbodiimide hydrochloride (EDC) (98%), N-hydroxysuccinimide (NHS) (98%), sodium azide (NaN$_3$, 98%) were from Aladdin. Sodium methacrylate (NaMA, 99%), ω-undecylenyl alcohol (98%), 2-bromoisobutyryl bromide (98%), 3-bromopropylamine hydrobromide (98%), and 4-morpholineethanesulfonic acid hydrate (MES) were from Alfa Aesar. N-Isopropylacrylamide (NIPAM, 99%), copper (I) bromide (CuBr, 98%), and pentamethyldiethylenetriamine (PMDETA, 98%) were from Aldrich. Glutaric acid, 2,2-dimethyl glutaric acid, 2,2-dimethyl succinic acid, and succinic acid were from TCI. PMAA (Mn 1100) and PAA (Mn 1300) were from Polymer Source Inc. Water (18 MΩ.cm) was from a Milli-Q Ultrapure water purification system.

Fourier-transform infrared spectrometry

A Bruker V80 spectrometer equipped with a deuterated triglycine sulfate (DTGS) detector was used to measure the spectra for the stepwise reactions. In all cases, samples were mounted in a vacuum chamber and thus the interference of CO$_2$ and water vapor from air was greatly attenuated. Spectra were recorded with 100 scans at a 7.5 kHz velocity and a resolution of 4 cm^{-1}, using a cleaned planar Si (100) chip as reference. All spectra were disposed with the OPUS software and spectral windows were zoomed to highlight the significant changes.

Preparation of porous silicon

The wafer was cut into 15×15×0.5 mm^3 pieces. Silicon chips were sonicated in ethanol, acetone and deionized water, each for 15 min.

Then, they were immersed in piranha solution (H_2SO_4/H_2O_2 (3/1 in v/v)) at the boiling temperature for 2 h to remove any organic residues. The cleaned chips were rinsed extensively with water and ethanol and subsequently dried in a stream of nitrogen (unless claimed, all the following chip cleaning and drying procedure adopted the steps). We used the metal-assisted stain etching to produce porous silicon.[7c] Briefly, the chip was immersed in 1% HF aqueous solution for 15 min to remove the surface silicon oxide film. After cleaning, the hydrided chip was deposited with a thin metallic film of Pt (10 nm thick) using a sputter-coater (SCD 500) at 15 mA for 180 s. The Pt-coated chip was etched in a mixture of 40% HF, 30% H_2O_2 and anhydrous ethanol with 2:2:1 (v/v/v) ratios for 4 min in dark and sequentially immersed in 1% HF aqueous solution for 1 min. Rinsed with copious water and ethanol and dried with N_2, hydrogen-terminated porous silicon chips were gained.

Surface hydrosilylation and introduction of surface initiator[4b,7c]

The freshly etched silicon chips were transferred into a glass bottle containing 10 mL neat ω-undecylenyl alcohol. The bottle was purged with N_2 for 15 min so as to vent the air. The reaction was performed in a CEM Discovery microwave reactor, controlled with a dynamic mode to reach 120 ^{0}C in 10 min and held there for 20 min. After reaction, the chip was washed sonically with anhydrous alcohol for 3 min and water for 3 min respectively. The undecylenyl alcohol-modified chip with hydroxy-termini was put into a glass bottle containing 10 mL CH_2Cl_2 and 2 mL Et_3N. The reaction vessel was cooled in an ice bath for 15 min, then 2 mL 2-bromoisobutyryl bromide was dropped in slowly, and finally the reaction solution stayed at room temperature for 12 h. After reaction, the chip with the surface initiator of 2-bromoisobutyryl groups was rinsed with copious CH_2Cl_2 and ethanol, dried with a mild nitrogen stream.

Preparation of PMAA and PMAA/PNIPAM brushes[4b,7c,9]

Surface-initiated polymerization of NaMA was performed in a N_2-filled vial with 1.69 g NaMA (15 mmol) and 75 μL PMDETA dissolved in a 5 mL solution of H_2O/ CH_3OH (1/1 in v/v). The solution was adjusted to pH 9.0. The bottle was purged with N_2 for 15 min so as to vent the air, followed by addition of 20 mg CuBr, and held at 40 ^{0}C for 5 h. Then, the chips were removed from the vial, washed with THF, H_2O and ethanol sequentially, and dried under a stream of N_2. PMAA brushes were obtained by immersion of the chip into 0.1 M phosphate-citric acid buffer (pH = 3.0) for 3 h to change carboxylate anions (COO^-) into carboxylic acid (COOH) species (The acidification procedure in the reiterative reactions followed the same protocol). The random polymer blend brushes of PMAA/PNIPAM were prepared with the same procedure. The total amount of monomers was 15 mmol. The 10 samples of random PMAA/PNIPAM blend brushes with different molar ratios of NIPAM:NaMA = 9:1, 8:2, 7:3, 6:4, 5:5, 4:6, 3:7, 2:8, 1:9 were prepared respectively.

Surface EDC/NHS activation of PMAA and PMAA/PNIPAM brushes

The EDC/NHS activation of the chip was performed with the optimum reaction condition reported previously by us,[4b] 0.1 mol/L EDC and 0.2 mol/L NHS in 0.1 mol/L MES buffer with pH 6.5 at room temperature for 1 h. After reaction, the chip was rinsed with water and dried under a stream of nitrogen.

EDC/NHS activation of dicarboxylic acids

The EDC/NHS activation of dicarboxylic acids of glutaric acid, 2,2-dimethyl glutaric acid, 2,2-dimethyl succinic acid, and succinic acid were performed with 0.1 mol/L dicarboxylic acid, 0.25 mol/L EDC,

and 0.25 mol/L NHS in 0.1 mol/L MES buffer (pH 6.5) at room temperature for 1 h. For example, 15 mL freshly prepared MES buffer containing 2.4 g EDC (0.0125 mol) was added immediately to a stirred 35 mL MES buffer containing glutaric acid (0.66 g, 0.005 mol) and NHS (1.44 g, 0.0125 mol) at 0 ^{0}C. Then the mixture was stirred at room temperature for 1 h. The white suspension was filtered, washed with water, then dissolved in dichloromethane, dried over anhydrous Na_2SO_4, and concentrated under vacuum. A white solid of glutaric acid di-succinimidyl ester (GA-NHS) was obtained after recrystallization from isopropyl alcohol (1.2 g, 73% yield). Following the same protocol, a white solid of 2,2-dimethyl glutaric acid di-succinimidyl ester (DMGA-NHS) was obtained after recrystallization with a yield of 85%. Whereas no products were obtained from either 2,2-dimethyl succinic acid or succinic acid solutions, following the same EDC/NHS activation protocol.

Preparation of 3-amino-1-azide propane (AAP)

AAP was prepared according to literature.[8] 3-Bromopropylamine hydrobromide (15 mmol, 3.2 g) was suspended in water (10 ml), followed by the addition of NaN_3 (50 mmol, 3.2 g) in 15 ml of water. The mixture was heated to 80 ^{0}C for 12 h, followed by the removal of 2/3 water in vacuum. The resulting mixture was cooled in an ice bath and diethyl ether (50 mL) and KOH pellets (4 g) were added while keeping the temperature <10 ^{0}C. The organic layer was separated and the aqueous phase was extracted with diethyl ether (2×30 mL), dried over K_2CO_3, and concentrated. The pure product was obtained by silica column with CH_3OH/CH_2Cl_2 (v:v = 1:3) to give a clear yellow oil (1.1 g, 73%).

Amidation

Generally the PMAA anhydride or NHS-ester chips were incubated in 5 mL 0.1 M $NaHCO_3/Na_2CO_3$ buffer (v/v = 1/1 with DMSO, pH = 8.5) containing 0.1 mM AAP at room temperature for 1 h, whereas for kinetic studies, the chips were taken out at 2, 20, 40, 80, and 120 min, rinsed with water and dried with nitrogen, and measured with the infrared spectrometer.

Results and Discussion

We have previously reported that the predominant product of EDC/NHS activation on PMAA is anhydride.[4] However, anhydride has its own weakness for amidation, only half carboxylic acids can be converted to amide, while the rest of halves return to carboxylic acids themselves, theoretically. To overcome this weakness, we reiterated the EDC/NHS activation for the rest of carboxylic acids and then amidation again three times. We define the products of the 1st, 2nd and 3rd EDC/NHS activations as **0.5G**, **1.5G**, and **2.5G** respectively, while the amidation products after **0.5G**, **1.5G**, and **2.5G** as **1.0G**, **2.0G** and **3.0G** respectively. Their respective infrared traces are shown in Fig. 1 and the infrared peak assignments in the carbonyl stretching region from 1500 to 2200 cm^{-1} are listed in Table S1 (see Table S1 in ESI).

The molar concentrations of surface species can be quantitatively estimated from their corresponding absorption bands by means of the Beer–Lambert law: $A = \varepsilon bc$ (where A is the absorbance, ε the molar extinction coefficient, b the thickness of polymer brushes, and c the concentration). To execute quantitative analyses using the infrared spectra in Fig. 1, we classified the reiterative reactions into two groups: **0.5G**, **1.5G**, **2.5G** and **1.0G**, **2.0G**, **3.0G**. In the first group, all three products in the infrared region of 1650~1850 cm^{-1}

COMMUNICATION   Journal Name

can be fitted as shown in the right column of Fig. 1: NHS-ester (associated pink triplex infrared bands at 1738, 1780, and 1811 cm^{-1}), anhydride (associated blue doublet bands at 1760 and 1802 cm^{-1}), and acid residue (green curved empty single band at 1714 cm^{-1}). Byproducts of N-acylurea will be ignored in the calculations because in the second group, non-trace in **1.0G** and neglectable trace in **2.0G** and **3.0G** of N-acylurea can be found in the carbonyl stretching region (1700~2000 cm^{-1}).[4b] The Beer–Lambert law for NHS-ester, anhydride, and acid in the first group can be written as:

$$A_{\text{NHS-ester}} = \varepsilon_{\text{NHS-ester}}bc_{\text{NHS-ester}}$$

$$A_{\text{anhydride}} = \varepsilon_{\text{anhydride}}bc_{\text{anhydride}}$$

$$A_{\text{acid}} = \varepsilon_{\text{acid}}bc_{\text{acid}}$$

where b has the same polymer thickness for all 3 species.

We adapted the linear relationship among the 3 individual molar extinction coefficients from our previous report: $\varepsilon_{\text{NHS-ester}}/\varepsilon_{\text{anhydride}}/\varepsilon_{\text{acid}} = 2 : 1.5 : 1$.[4b] The largest peak heights of each species in Fig. 1 were used as the absorbance (A) for calculations: 1760 cm^{-1} for anhydride, 1738 cm^{-1} for NHS-ester, and 1714 cm^{-1} for carboxylic acid, individually.

Assuming all reactants of the side chain acid groups are converted to NHS-ester, anhydride, acid residue, and not to any other compounds, then the molar percentages (represented with β) with an acid group as the unit converting to NHS-ester ($\beta_{\text{NHS-ester}}$), anhydride ($\beta_{\text{anhydride}}$), and acid (β_{acid}) can be calculated individually in equations 1~3.

$$\beta_{\text{NHS-ester}} = \frac{A_{\text{NHS-ester}}/\varepsilon_{\text{NHS-ester}}}{A_{\text{NHS-ester}}/\varepsilon_{\text{NHS-ester}} + 2A_{\text{anhydride}}/\varepsilon_{\text{anhydride}} + A_{\text{acid}}/\varepsilon_{\text{acid}}}100\% \tag{1}$$

$$\beta_{\text{anhydride}} = \frac{2A_{\text{anhydride}}/\varepsilon_{\text{anhydride}}}{A_{\text{NHS-ester}}/\varepsilon_{\text{NHS-ester}} + 2A_{\text{anhydride}}/\varepsilon_{\text{anhydride}} + A_{\text{acid}}/\varepsilon_{\text{acid}}}100\% \tag{2}$$

$$\beta_{\text{acid}} = \frac{A_{\text{acid}}/\varepsilon_{\text{acid}}}{A_{\text{NHS-ester}}/\varepsilon_{\text{NHS-ester}} + 2A_{\text{anhydride}}/\varepsilon_{\text{anhydride}} + A_{\text{acid}}/\varepsilon_{\text{acid}}}100\% \tag{3}$$

We obtained $\beta_{\text{anhydride}}$, $\beta_{\text{NHS-ester}}$, β_{acid} as 83, 10, 7; 52, 28, 20; 17, 46, 37 for **0.5G**, **1.5G**, and **2.5G** respectively (see Table S2 in ESI).

For the second group of **1.0G**, **2.0G**, and **3.0G**, there are only two products of amide and carboxylate, which can be proven from their respective infrared traces in Fig. 1. Amide was confirmed with amide I and II at 1650 and 1529 cm^{-1} respectively. Since the weak amide II overlaps with carboxylate (1570 cm^{-1}) and amide I is always complicated by environments such as water vapor and its orientation in the supporting substrate,[10] we used the independent and strong vibration band of azide at 2105 cm^{-1}, plus carboxylate (1570 cm^{-1}), to calculate the amide yield (α_{azide}) as follows:

$$A_{\text{azide}} = \varepsilon_{\text{azide}}bc_{\text{azide}} \qquad A_{\text{coo}^-} = \varepsilon_{\text{coo}^-}bc_{\text{coo}^-}$$

$$\alpha_{\text{azide}} = \frac{c_{\text{azide}}}{c_{\text{azide}} + c_{\text{COO}^-}}100\% = \frac{\dfrac{A_{\text{azide}}}{\varepsilon_{\text{azide}}}}{\dfrac{A_{\text{azide}}}{\varepsilon_{\text{azide}}} + \dfrac{A_{\text{COO}^-}}{\varepsilon_{\text{COO}^-}}}100\% \tag{5}$$

where A_{azide} and A_{COO^-} can be obtained from the peak heights of 2105 and 1570 cm^{-1} in Fig. 1 respectively. We adapted the molar extinction coefficients of $\varepsilon_{\text{azide}} = 1000$ LM^{-1}cm^{-1} [11] and $\varepsilon_{\text{COO}^-} = 380$ LM^{-1}cm^{-1} [12] from previous reports, therefore the amide yields were obtained for **1.0G**, **2.0G**, and **3.0G** as 32, 48, and 62% respectively. Combining both calculated results of $\beta_{\text{anhydride}}$, $\beta_{\text{NHS-ester}}$, β_{acid} and

α_{azide}, we can easily derive the component compositions (see Table S3 in ESI) shown in Scheme 1 under their corresponding structures respectively.

The molecular structures and their stoichiometric molar ratios shown in Scheme 1 are derived from the quantitative analyses of infrared spectra. Details are illustrated: i) During the first EDC/NHS activation (**0.5G**), anhydride is the overwhelming product (83%), due to the faster kinetic ring-closing mechanism and the thermodynamically stable anhydride; then the left lonely acid side chains are partly esterified to NHS-ester (10%) and partly left as unreacted acid residues (7%), due to steric hindrance, such as the one-end fixed backbone on silicon having less freedom of translation and rotation. ii) Successive AAP amidation (**1.0G**) generates amides (32%) and carboxylates (68%), which can be assigned to three subunit structures. The green subunit can be inferred statistically if amidation occurs in an even space when half of anhydrides react with AAP. Supposing that NHS-ester converts completely to amide and other chemical conversions rationally follow the dash arrows from **0.5G** to **1.0G**, an algebraic approach for balancing the chemical equation gives perfectly matching compositions for the subunit structures depicted in **1.0G**, among which the green subunit is the key structure to interpret the reaction mechanisms self-consistently. iii) For the 2nd EDC/NHS activation (**1.5G**), the independently measured molar percentages of anhydride (35%), NHS-ester (19%), and acid (14%), follow the chemical reaction logistics from **1.0G** perfectly. vi) Successive amidation (**2.0G**) produces amides (48%) and carboxylates (52%). v) The 3rd EDC/NHS activation (**2.5G**) of the left 48% acids provides anhydride (9%), NHS-ester (24%), and acid (19%). vi) Successive AAP amidation generates amides (62%) and carboxylate residues (38%). Repeating the EDC/NHS activation further will generate overwhelming NHS-ester intermediates and the AAP amidation further will achieve over 80% amides. All subunits depicted as monomers are suggested rationally and inferred from the green subunits logistically.
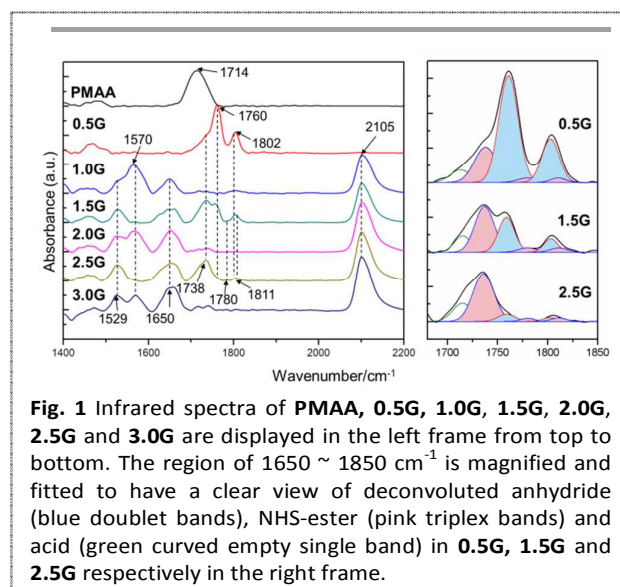
Fig. 1 Infrared spectra of **PMAA, 0.5G, 1.0G, 1.5G, 2.0G, 2.5G** and **3.0G** are displayed in the left frame from top to bottom. The region of 1650 ~ 1850 cm^{-1} is magnified and fitted to have a clear view of deconvoluted anhydride (blue doublet bands), NHS-ester (pink triplex bands) and acid (green curved empty single band) in **0.5G, 1.5G** and **2.5G** respectively in the right frame.

From the above self-consistent quantitative analyses, we can deduce the key idea about the structure-reactivity relationship: All

acid side chains standing next to each other will form anhydride primarily due to Thorpe-Ingold effect, unless they are sterically hindered. While the lonely acid side chains isolated by others, and acid side chains acting as lonely ones such as in trimer after anhydride formation at either side or in tetramer after anhydride formation at the middle, form NHS-ester.

To prove the above structure-reactivity statement further, we applied the EDC/NHS activations on another PMAA-based acid system, random polymer blends of PMAA/PNIPAM with a series of molar blending ratios of 10, 20, 30, 40, 50, 60, 70, 80, 90, 100% PMAA at an increasing concentration step of 10% PMAA. In the polymer blends, methacrylic acids are interrupted by N-
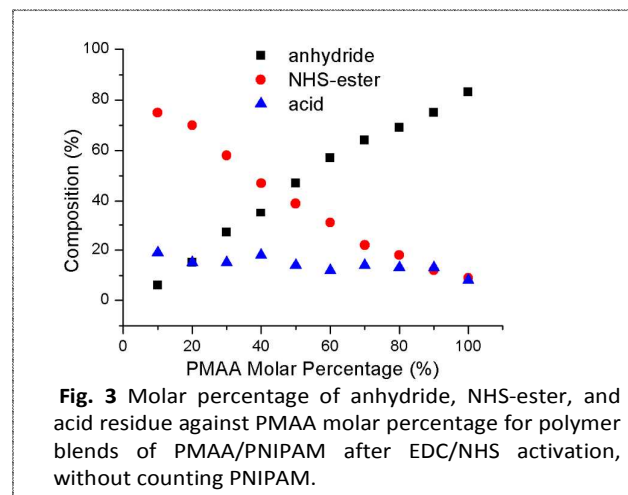
isopropylacrylamide monomers or oligomers into monomers, dimers, trimers, and multimers sequentially and statistically from low to high PMAA concentrations in the backbone. After EDC/NHS activation, we observed the similar evolution phenomena for both products of NHS-ester and anhydride in Fig. 2: with decreasing the molar concentration of PMAA from 100% to 10%, anhydride evolves from dominant to recessive, while NHS-ester from recessive to dominant.

Fig. 2 Infrared spectra of the EDC/NHS activated polymer blends of PMAA/PNIPAM with molar blending ratios of 10, 20, 30, 40, 50, 60, 70, 80, 90, 100% PMAA respectively. The two intermediates of NHS-ester (associated triplex bands at 1738, 1780, 1807 cm^{-1}) and anhydride (associated doublets at 1760 and 1804 cm^{-1}) and the acid residue (1717 cm^{-1}) are indicated. Amide I at 1652 cm^{-1} and amide II at 1535 cm^{-1} are from PNIPAM. A few wavenumber shifts of the same species from Fig. 1 are due to different neighboring group effects.

Quantitative analysis for Fig. 2 with equations 1~3 after deconvolution (ignored) of the 10 traces in the infrared region of 1700 ~ 1900 cm^{-1} provide the product composition against PMAA molar percentage in Fig. 3, without counting PNIPAM. Obviously, 10~20% acid residues remain un-reacted, which is rational from the knowledge of chemical reactions; anhydride increases with PMAA concentrations roughly in a linear relationship, from 6% in 10% PMAA/PNIPAM blend up to 83% in pure PMAA; while NHS-ester,

Scheme 1 Schematic drawing of molecular structures with three reiterative EDC/NHS activations and amidations of PMAA (molar percentages are listed under the subunit structures respectively). The structures in parentheses are subunits while in brackets the units for the polymer blend. Curved lines represent connections, but not only in this order; subunits in parentheses with alphabet subscripts of m, n, p, k (≥ 1) are variable in integers, meaning they can be lonely or next to each other, while subunits in parentheses without subscripts indicate they are lonely and cannot be next to each other themselves. **0.5G**, **1.5G**, **2.5G** represent the products after the 1st , 2nd and 3rd EDC/NHS activations respectively; **1.0G**, **2.0G**, and **3.0G** represent the products after successive amidations following **0.5G**, **1.5G**, **2.5G** sequentially.

Fig. 3 Molar percentage of anhydride, NHS-ester, and acid residue against PMAA molar percentage for polymer blends of PMAA/PNIPAM after EDC/NHS activation, without counting PNIPAM.
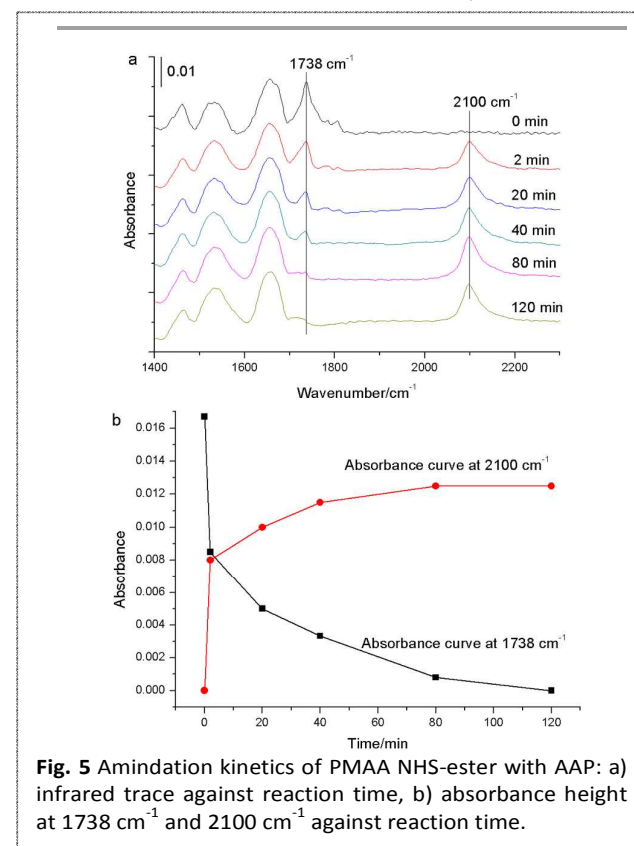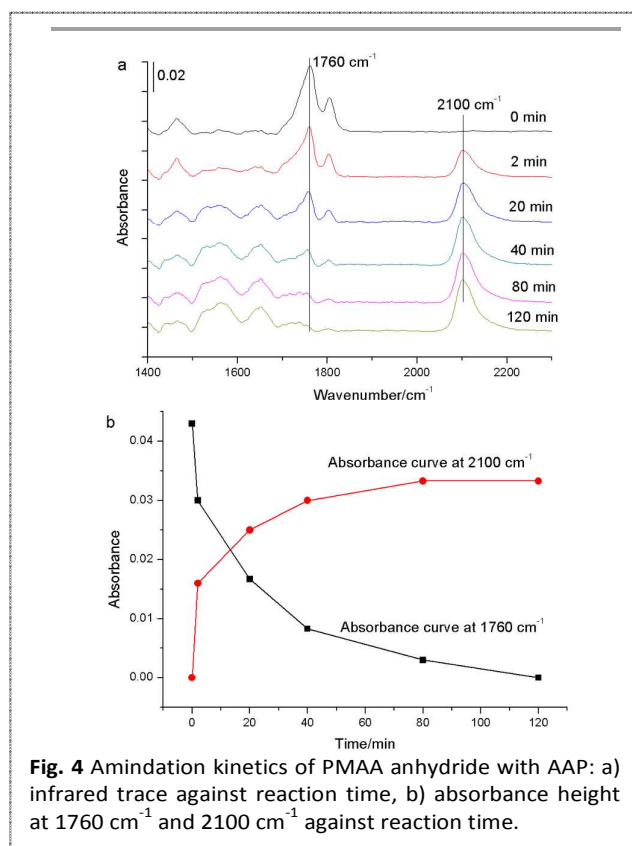
contrast to anhydride, decreases, linearly, from 76% in 10% PMAA/PNIPAM blend to 9% in pure PMAA. In the medium PMAA concentration range (30~70%), both anhydride and NHS-ester are generated in considerable quantities. The observed phenomena can be explained as the same as that for the reiterative EDC/NHS activations on PMAA brushes. Lonely acid side chains are dominant at lower PMAA concentrations, oligomers of MAA such as dimers, trimers, and tetramers are the major structures of PMAA in the medium concentration range, while multimers (≥4) become the overwhelming structures at higher PMAA concentrations. Such structural distributions result in the complementary waxing of NHS-ester and waning of anhydride with fragmentation of PMAA in the polymer blend.

From the above qualitative and quantitative analysis of the infrared traces, we suggest the following mechanism for EDC/NHS activation of PMAA: the acid side chain next to itself in multimer or even in dimer of a polymer chain will form anhydride primarily, and the lonely acid side chain isolated by others will convert to NHS-ester.

Amidation kinetics

We have demonstrated the EDC/NHS activation product details of PMAA with different contents in its random polymer blends. While the main goal of EDC/NHS activation of carboxylic acids is to couple free amine-containing biomolecules, what is the kinetic behavior of PMAA anhydride or NHS-ester during the amidation process? To compare their kinetics, we used an anhydride, directly derivatised from PMAA brushes with a dominant content of ~80% in all acid derivatives, and an NHS-ester derivatised from a 30% PMAA-

containing PMAA/PNIPAM blend with a content of ~60% in all acid derivatives, as examples to run the kinetic experiments with AAP. Although a higher NHS-ester content over 70% in all acid derivatives can be derivatised from the 20% or less PMAA-containing PMAA/PNIPAM blend, the absolute amount of NHS-ester is too low to precisely assay the amidation kinetics, therefore we preferred to use NHS-ester from a 30% PMAA-containing PMAA/PNIPAM blend. Figure 4 illustrated the amidation kinetics of PMAA anhydride, where Figure 4a demonstrated the spectral evolution over time and Figure 4b drew the absorbance curve of the height at 1760 cm^{-1} and 2100 cm^{-1} versus time, indicating the anhydride consuming rate and the amide formation rate respectively. Similarly, Figure 5 presented the amidation kinetics of NHS-ester in the PMAA/PNIPAM blend containing 70% PNIPAM with strong and broad amide bands at 1652 cm^{-1} and 1535 cm^{-1}, where Figure 5a demonstrated the spectral evolution over time and Figure 5b drew the absorbance curve of the height at 1738 cm^{-1} and 2100 cm^{-1} versus time, indicating the NHS-ester consuming rate and the amide formation rate respectively. From both Figures 4 and 5, we concluded that their amidation kinetics were similar. More details are sumarised: (1) At the first 2 min, the amidation reactions were very fast, 50% and 64% amidation products were obtained for anhydride and NHS-ester respectively, whereas 30% anhydride and 50% NHS-ester were consumed. (2) As time went on to 40 min, both of the amidation reactions were close to completion, therefore the reaction time of 1 h was adequate for termination of amidation reactions. (3) Trace amount of residues of anhydrides or NHS-esters at even 80 min should be due to the buried species within the

Fig. 4 Amindation kinetics of PMAA anhydride with AAP: a) infrared trace against reaction time, b) absorbance height at 1760 cm^{-1} and 2100 cm^{-1} against reaction time.

Fig. 5 Amindation kinetics of PMAA NHS-ester with AAP: a) infrared trace against reaction time, b) absorbance height at 1738 cm^{-1} and 2100 cm^{-1} against reaction time.

Journal Name COMMUNICATION

polymer brushes, which would be mainly hydrolysed late because they were more likely surrounded by water molecules. (4) Hydrolysis as a competitive reaction is much slower than amidation at pH 8.5, for both PMAA anhydride and NHS-ester, since the water molecule is a weaker nucleophile than the primary amine during the nucleophilic substitution reaction. Generally, most of anhydrides are much less stable than NHS-ester and therefore will be hydrolysed immediately at aqueous media, whereas PMAA anhydride possesses a stable structure duo to the gem-dialkyl group effect, therefore it proceeds through a slow hydrolysis over hours in weak alkaline solutions, comparable to NHS-ester.

EDC/NHS activation of glutaric acids and succinic acids

Since the anhydride formation in the EDC/NHS activation of PMAA is due to the Thorpe-Ingold effect: the side methyl groups compress the acid side chains close to each other, therefore the formation six-membered anhydride ring by the nucleophilic attack of the intramolecular neighboring acid is much faster than any other pathways for derivatisation of O-acylisourea; while for PAA, the neighboring acid distance should be a little bit longer than that in PMAA, its dominant product is NHS-ester but not anhydride, due to the faster nucleophilic attack on O-acylisourea from NHS rather than from a neighboring acid.[4] Does the Thorpe-Ingold effect also play a role for small molecules in the EDC/NHS activation reaction, with analoguous structures to the MAA dimer in PMAA? We ran the EDC/NHS reactions for 4 available dicarboxylic acids: glutaric acid, 2,2-dimethyl glutaric acid, succinic acid, and 2,2-dimethyl succinic acid. The di-NHS-ester products (GA-NHS[13] and DMGA-NHS, their IR, ^{1}H-NMR and MS are in Figs. S1-5 of ESI) were easily obtained for glutaric acid and 2,2-dimethyl glutaric acid, as white precipitates in Fig. S1; whereas the di-NHS-ester products were not observed for succinic acid and 2,2-dimethyl succinic acid, the reaction solutions were clear and the acids remained unreacted. Why do the similar dicarboxylic acids exhibit such different products? From our understanding on the EDC/NHS activation of PMAA and PAA, we give our interpretation here to coordinate the observed phenomena together: The distance between two end carboxylic acids in glutaric acid and 2,2-dimethyl glutaric acid is a little bit longer than in succinic acid and 2,2-dimethyl succinic acid, once an O-acylisourea is formed, the nucleophilic attack competition between NHS and the neighboring acid on O-acylisourea determines the final product. For glutaric acid and 2,2-dimethyl glutaric acid, the nucleophilic attack from NHS is faster than from its neighboring acid, therefore di-NHS-ester products are formed easily with high yields. While for succinic acid and 2,2-dimethyl succinic acid, the nucleophilic attack from its neighboring acid is faster than from NHS due to the Thorpe-Ingold effect, therefore the five-membered ring anhydride, succinic or 2,2-dimethyl succinic anhydride, forms primarily. However both succinic anhydride and 2,2-dimethyl succinic anhydride are so vulnerable in aqueous media, they will be hydrolysed to acids immediately. Both O-acylisourea and succinic anhydrides can react with NHS thermodynamically, however the kinetic probability of the NHS attack cannot compete with its competitors. Therefore the formation and hydrolysis of succinic anhydrides during the EDC/NHS activation forms a cycle. By the end, the only consumed reactants are EDC and water, which follows the 4th pathway as described in Introduction: O-acylisourea

was hydrolysed to urea and carboxylic acid by consuming carbodiimide only.

By the way, ideal small dicarboxylic acid molecules, for investigation of the gem-dialkyl effect in the EDC/NHS activation, will be the gem-dialkyl glutaric acid, i.e. 2,2,4,4-tetramethyl glutaric acid and 2,4-dimethyl-2,4-diethyl glutaric acid, resembling the MAA dimer structure in PMAA better. However these small molecules have not yet been synthesized, maybe due to the crowded side groups.

Discussion

From the above experimental results, we infer that, in the analogous structures of glutaric acids including PMAA and PAA, the initial EDC activation of the carboxylic acid to O-acylisourea is a slow step, then the conversion of O-acylisourea to NHS-ester (the 1st pathway) or to anhydride (the 2nd pathway) is a fast step. Formation of either NHS-ester or anhydride depends on the competition of nucleophilic attack from a neighboring acid or from NHS. The gem-dialkyl groups in PMAA demonstrated the typical Thorpe-Ingold effect in the EDC/NHS activation, that a little bit shorter distance between neighboring acid groups brought by the gem-dialkyl groups in PMAA resulted in the faster nucleophilic attack on O-acylisourea from its neighboring acid and therefore generated anhydride. Whereas for PAA, the nucleophilic attack on O-acylisourea from NHS was faster than its neighboring acid, thus the dominant EDC/NHS activation product was NHS-ester.[4b] It is also reasonable to deduce that the 3rd conversion pathway of O-acylisourea to a stable side product of N-acyl urea by intramolecular rearrangement and the 4th pathway of hydrolysis of O-acylisourea by water attack would be slower than the 1st and 2nd pathways. To precisely measure and distinguish the in-situ kinetics of formation of NHS-ester, or anhydride in molecular level is beyond the scope of our experimental skills. However we adapted a very rough analysis approach to demonstrate their kinetic difference at the macroscale by following the precipitation rate of PMAA anhydride and the one of PAA NHS-ester with measurement of the optical density (OD) at 600 nm in Figs. S6 and S7. We observed that PMAA anhydride precipitated immediately after the addition of EDC to the reaction solution of PMAA and NHS, and the optical density of the solution achieved saturation of 0.8 OD at 240 sec (or 4 min). It was very likely that the OD saturation meant the completion of the reaction. While for the precipitation of PAA NHS-ester, it started to precipitate at 120 sec (or 2 min) after the addition of EDC, and the precipitation became slower after 360 sec (or 6 min) and still continued very slowly until our measurement time window of 1000 sec (or ~17 min). All the above experimental results, including the precipitation rate measurements, render us to suggest that the formation of either anhydride or NHS-ester depends on the nucleophilic attack kinetics on O-acylisourea from the intramolecular neighboring acid or from the intermolecular NHS, in the molecular level. Therefore, except for the succinic acid and gem-dialkyl glutaric acid structures which can be affected by the Thorpe-Ingold effect obviously, all other alkyl acids with a distance between two adjacent acids longer than glutaric acid will form the dominant intermediate product of NHS-esters.

Conclusion

COMMUNICATION

In conclusion, for the irregular EDC/NHS activation products of PMAA, we observed the waxing of NHS-ester and the waning of anhydride with increasing the fragmentation degree of PMAA blocks in PMAA-associated polymer blends. It is the delicate kinetics and thermodynamics in the molecular level that bring the complicated production results in the macroscale world, such as variable products and yields for different kinds of acids. Our finding of the different EDC/NHS activation products between PMAA and PAA and the following understanding of the Thorpe-Ingold effect on the EDC/NHS activation of PMAA rendered us to explain the complementary waxing of NHS-ester versus the waning of anhydride phenomena clearly. Although the Thorpe-Ingold effect is the key to interpret the observed phenomena, steric hindrance should also be included, especially for the small part of NHS-ester in the pure PMAA, and for nontrivial NHS-esters in PMAA oligomers such as dimer, trimer, tetramer, etc. From our above speculations about the EDC/NHS activation kinetics, we would suggest some modifications for the well-known EDC/NHS reaction recipes used widely. For example, the molar ratios of EDC/NHS/acid = 1.2:1.2:1, in general reaction conditions, are commonly accepted, whereas we suggest to add more additives of NHS, i.e. 2 to 5 or even more folds to acid, in the reaction to obtain NHS-ester with higher yield, since more NHS molecules will increase the probability of their nucleophilic attack on O-acylisourea. Since the EDC/NHS activation of PMAA is so popularly used for biomolecular immobilization and conjugation in biomaterials, pharmaceuticals, immunology, and food science, such a clear understanding of the reaction mechanism suggests how to load more biomolecules while save money. Only EDC and not any other additives such as NHS or HOBt is needed at the first reaction to activate PMAA and synthesize amide linkages, and then reiterating the EDC/NHS activation and amidation on the product from the first round will increase the amidation efficiency dramatically. We believe more precise experimental measurements and theoretical studies of the EDC/NHS acitivation mechanisms, both in kinetics and thermodynamics, will help to resolve the ambiguity of the carbodiimide/additive coupling reaction for amide bond formation better.

Notes and references
1   (a) A. Williams, T. I. Ibrahim, *Chem. Rev.* 1981, **81**, 589. (b) V. R. Pattabiraman, J. W. Bode, *Nature* 2011, **480**, 471. (c) L. H. H. Olde Damink, P. J. Dijkstra, M. J. A. van Luyn, P. B. van Wachem, P. Nieuwenhuis, J. Feijen, *Biomaterials* 1996, **17**, 765. (d) C. A. G. N. Montalbetti, V. Falque, *Tetrahedron* 2005, **61**, 10827. (e) M. M. Joullié, K. M. Lassen, *Arkvoc* 2010, 189. (f) Z. Grabarek, J. Gergely, *Anal. Biochem.* 1990, **185**, 131. (g) M. J. B. Wissink, R. Beernink, J. S. Pieper, A. A. Poot , G. H. M. Engbers, T. Beugeling, W. G. van Aken, J. Feijen, *Biomaterials* 2001, **22**, 151. (h) J. V. Staros, R. W. Wright, D. M. Swingle, *Anal. Biochem.* 1986, **156**, 220.
2   (a) T. Iwasawa, P. Wash, C. Gibson, J. Jr. Rebek, *Tetrahedron* 2007, **63**, 6506. (b) N. Nakajima, Y. Ikada, *Bioconjugate Chem.* 1995, **6**, 123. (c) B. M. Prentice, J. D. Gilbert, J. R. Stutzman, W. P. Forrest, S. A. McLuckey, *J. Am. Soc. Mass Spectrom.* 2013, **24**, 30.
3   (a) D. F. De Tar, R. Silverstein, *J. Am. Chem. Soc.* 1966, **88**, 1013. (b) D. F. De Tar, R. Silverstein, *J. Am. Chem. Soc.* 1966, **88**, 1020.
4   (a) H.B. Liu, Q. Yan, C. E. Wang, X. Liu, C. Wang, X. H. Zhou, S. J. Xiao, *Colloids Surf. A* 2011, **386**, 131. (b) C. Wang, Q. Yan, H. B. Liu, X. H. Zhou, S. J. Xiao, *Langmuir* 2011, **27**, 12058.
5   (a) M. R. Lockett, M. F. Phillips, J. L. Jarecki, D. Peelen, L. M. Smith, *Langmuir* 2008, **24**, 69. (b) R. L. Touahir, J.-N. Chazalviel, S. Sam, A. Moraillon, C. Henry de Villeneuve, P. Allongue, F. Ozanam, A. C. Gouget-Laemmel, *J. Phy. Chem. C* 2011, **115**, 6782. (c) S. Sam,; L. Touahir, J. S. Andresa, P. Allongue, J. N. Chazalviel, A. C. Gouget-Laemmel, C. Henry de Villeneuve, A. Moraillon, F. Ozanam, N. Gabouze, S. Djebba, *Langmuir* 2010, **26**, 809. (d) C. Y. Lim, N. A. Owens, R. D. Wampler, Y. Ying, J. H. Granger, M. D. Porter, *Langmuir* 2014, **30**, 12868. (e) F. Palazon, C. M. Benavides, D. Leonard, E. Souteyrand, Y. Chevolot, J. P. Cloarec, *Langmuir* 2014, **30**, 4545.
6   (a) R. M. Beesley, C. K. Ingold, J. F. Thorpe, *J. Chem. Soc., Trans.* 1915, **107**, 1080. (b) M. E. Jung, G. Piizzi, *Chem. Rev.* **2005**, *105*, 1735. (c) C. Galli, L. Mandolini, *Eur. J. Org. Chem.* 2000, 3117. (d) C. Galli, L. Mandolini, *Acc. Chem. Res.* 1981, **14**, 94. (e) R. Salvio, L. Mandolini, C. Savelli, *J. Org. Chem.* 2013, **78**, 7259.
7   (a) H. F. Li, H. M. Han, Y. G. Wu, S. J. Xiao, *Appl. Surf. Sci.* 2010, **256**, 4048. (b) C. Wang, X. M. Jia, C. Jiang, G. N. Zhuang, Q. Yan, S. J. Xiao, *Analyst*, 2012, **137**, 4539. (c) M. Xiao, H. M. Han, S. J. Xiao, *Sci. China Chem.* 2013, **56**, 1152.
8   N. S. Hatzakis, H. Engelkamp, K. Velonia, J. Hofkens, P. C. Christianen, A. Svendsen, S. A. Patkar, J. Vind, J. C. Maan, A. E. Rowan, R. J. Nolte, *Chem. Commun.* 2006, 2012.
9   S. Tugulu, R. Barbey, M. Harms, M. Fricke, D. Volkmer, A. Rossi, H. A. Klok, *Macromolecules* 2007, **40**, 168.
10 (a) S. J. Xiao, S. Brunner, M. Wieland, *J. Phys. Chem. B* 2004, **108**, 16508. (b) S. J. Xiao, M. Wieland, S. Brunner, *J. Colloid Interf. Sci.* 2005, **290**, 172.
11 I. T. Suydam, S. G. Boxer, *Biochemistry*, 2003, **42**, 12050.
12 A. Barth, *Prog. Biophys. Mol. Biol.* 2000, **74**, 141.
13 T. A. van den Berg, B. L. Feringa, G. Roelfes, *Chem. Commun.* 2007, 180.